Computational Screening of Metal-Organic Frameworks for Xenon/Krypton Separation

Patrick Ryan
Dept. of Chemical and Biological Engineering, Northwestern University, Evanston, IL 60208

Omar K. Farha
Dept. of Chemistry, Northwestern University, Evanston, IL 60208

Linda J. Broadbelt and Randall Q. Snurr
Dept. of Chemical and Biological Engineering, Northwestern University, Evanston, IL 60208

DOI 10.1002/aic.12397
Published online September 24, 2010 in Wiley Online Library (wileyonlinelibrary.com).

A variety of metal-organic frameworks (MOFs) with varying linkers, topologies, pore sizes, and metal atoms were screened for xenon/krypton separation using grand canonical Monte Carlo (GCMC) simulations. The results indicate that small pores with strong adsorption sites are desired to preferentially adsorb xenon over krypton in multicomponent adsorption. However, if the pore size is too small, it can significantly limit overall gas uptake, which is undesirable. Based on our simulations, MOF-505 was identified as a promising material due to its increased xenon selectivity over a wider pressure range compared with other MOFs investigated. © 2010 American Institute of Chemical Engineers *AIChE J,* 57: 1759–1766, 2011
Keywords: adsorption/gas, simulation, molecular, thermodynamics/statistical

Introduction

Separating xenon from krypton is an industrially important problem. Xenon and krypton are used in fluorescent light bulbs, and current technology produces these gases from the cryogenic distillation of air in which these noble gases are present in small concentrations (1.14 ppmv Kr, 0.086 ppmv Xe). Both xenon and krypton separate into the oxygen-rich stream after distillation, and these gases are concentrated and purified to produce an 80/20 molar mixture of krypton to xenon.[1] This final mixture typically undergoes further cryogenic distillation to produce pure krypton and pure xenon. Distillation is an energy-intensive process, and separation of these gases by selective adsorption near room temperature would be more energy efficient. Additionally, separating krypton from xenon is an important step in removing radioactive ^{85}Kr during treatment of spent nuclear fuel.[2] However, even after cryogenic distillation, trace levels of radioactive krypton in the xenon-rich phase are too high to permit further use.[2] If adsorbents could reduce ^{85}Kr concentrations in the xenon-rich phase to permissible levels, there could be an entirely new supply source of xenon for industrial use. Thus, there is a strong need to develop adsorbent materials for this separation to reduce energy consumption and to reuse byproducts of consumed nuclear fuel.

There are several examples in the literature in which zeolites have been tested for Xe/Kr separation. Previous research has shown NaX zeolite to be a selective adsorbent for xenon over krypton with a selectivity of approximately six with krypton concentrations ranging from 1 to 10,000 ppm.[2] Jameson et al.[3] showed that NaA zeolite had a selectivity of approximately four for binary mixtures of xenon and krypton at 300 K between 0.1 and 1 MPa. They also used molecular simulations to show that ideal adsorbed solution theory (IAST) could accurately predict the selectivities and mixture behavior from the single-component isotherms.

Additional Supporting Information may be found in the online version of this article.

Correspondence concerning this article should be addressed to R. Q. Snurr at snurr@northwestern.edu.

Table 1. Pore Diameters of All MOFs Investigated Estimated from Pore Size Distribution Calculations

MOF	Pore Sizes (nm)		
IRMOF-1	1.12	1.45	
UMCM-1	1.03	1.39	2.33
ZIF-8	1.05		
HKUST-1	0.50	1.06	1.24
MOF-505	0.48	0.71	0.95
NOTT-101	0.50	0.96	1.05
NOTT-108	0.45	0.89	1.05
Pd-MOF	0.22	0.49	0.58

Metal-organic frameworks,[4–6] or MOFs, are a new class of nanoporous materials. Composed of organic linkers and metal corners, these materials self-assemble in solution to form stable, crystalline frameworks. Coordination bonds between oxygen and nitrogen atoms with metal centers allow for a variety of topologies, and choice of the organic linker allows one to tailor pore sizes and environments for particular applications. As a result, these materials have garnered much attention for hydrogen storage,[7–9] separations,[10,11] and catalysis.[12–14]

A number of groups have investigated MOFs for separation. For example, Bae et al.[15] used both experiments and simulation to show that a mixed-ligand MOF can separate carbon dioxide from methane. Bae et al.[16] also showed that exchanging fluorinated-methylpyridine into a MOF could substantially increase the selectivity of carbon dioxide over nitrogen due to the increased polar environment. Pan et al.[17] synthesized a microporous MOF with 1D hydrophobic microchannels and demonstrated its ability to separate *n*-butane from other *n*-alkanes and olefins. Hartmann et al.[18] showed that isobutene can be separated from isobutane using HKUST-1 in a breakthrough system. Yang et al.[19,20] used molecular simulations to predict that HKUST-1 is a promising candidate for separation of carbon dioxide from both air and methane/hydrogen mixtures.

To date, there are a few publications that report the investigation of Xe/Kr separation using MOFs. Mueller et al.[21] measured noble gas adsorption in IRMOF-1 and noticed significantly higher adsorption for xenon and krypton in MOF-filled containers relative to containers without MOF material. Building on these results, they built a breakthrough system filled with HKUST-1 and showed that a 94/6 molar mixture of krypton/xenon could be purified to over 99% krypton and less than 50 ppm xenon. Recently, Greathouse et al.[22] simulated noble gas adsorption in IRMOF-1. They predicted that IRMOF-1 has a selectivity of approximately 2.5–3 for Xe over Kr at 298 K and pressures of both 0.1 and 1 MPa.

In this article, we screened computationally a variety of MOFs with different pore sizes for xenon/krypton separation to maximize selectivity. Additionally, we aimed to determine the separation mechanism of HKUST-1, which was previously shown to be an effective adsorbent for this separation. Finally, we sought to delineate which material properties are desirable to develop even more selective materials for this separation.

Methods

We chose a number of MOFs with different pore sizes, linkers, metal atoms, and topologies to sample a variety of MOF properties and gain insight into which characteristics are desired for Xe/Kr separation. The selected MOFs are IRMOF-1,[23] UMCM-1,[24] ZIF-8,[25] HKUST-1,[26] MOF-505,[27] NOTT-101,[28] NOTT-108,[28] and Pd-MOF.[29] We have calculated the pore size distribution for each of these MOFs (see Supporting Information for graphs), and the results are summarized in Table 1. IRMOF-1 is composed of Zn_4O corners and benzenedicarboxylate (BDC) linkers and has large pore diameters of 1.12 and 1.45 nm. UMCM-1 also has Zn_4O corners but has two organic linkers: BDC and 1,3,5-tris(4-carboxyphenyl)benzene. This MOF contains both microporous and mesoporous cavities. Zeolitic-imidazolate-framework #8 (ZIF-8) contains tetrahedral Zn^{2+} atoms coordinated to methylimidazolate linkers in a sodalite-type framework. Its main cavity spans 1.05 nm across. HKUST-1 is made of copper paddlewheels with benzenetricarboxylate linkers, which form both small and large pockets. The smaller pockets have diameters of 0.50 nm, whereas the larger cavities have diameters of 1.06 and 1.24 nm. The window into these small pockets is ~0.46 nm, and previous experimental work using ^{129}Xe NMR spectroscopy[30] has demonstrated that these sites are accessible to xenon. Based on the size of krypton and xenon, whose Lennard-Jones diameters are 0.3636 and 0.4100 nm, respectively, these pockets should be accessible as adsorption sites. MOF-505 is composed of Cu^{2+} paddlewheels coordinated to biphenyltetracarboxylate linkers. Similar to MOF-505, NOTT-101 uses Cu^{2+} paddlewheels with triphenyl tetracarboxylate linkers and results in slightly larger pores of 0.50, 0.96, and 1.05 nm. NOTT-108 is identical to NOTT-101 with the exception of four fluorine atoms in the place of hydrogens on the middle phenyl moiety of the triphenyl linker. As the NOTT-101 crystal structure was not published in the original article, we constructed a NOTT-101 structure by using the NOTT-108 structure and manually changing fluorine atoms to hydrogen atoms and adjusting the carbon-fluorine bond lengths. Pd-MOF contains Pd^{2+} cations bonded to 2-hydroxypyrimidinolate linkers in a sodalite topology. The coordinated Pd atoms exist in a square planar configuration, and the MOF has pore diameters of ~0.22, 0.49, and 0.58 nm.

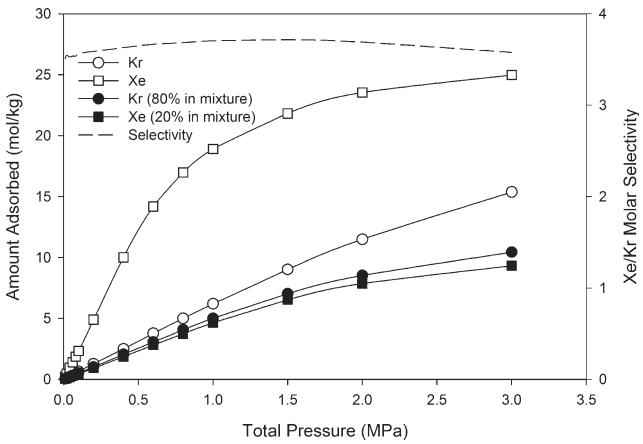

Figure 1. Single-component (open symbols) and mixture (filled symbols) isotherms for Xe and Kr adsorption in UMCM-1 at 273 K.

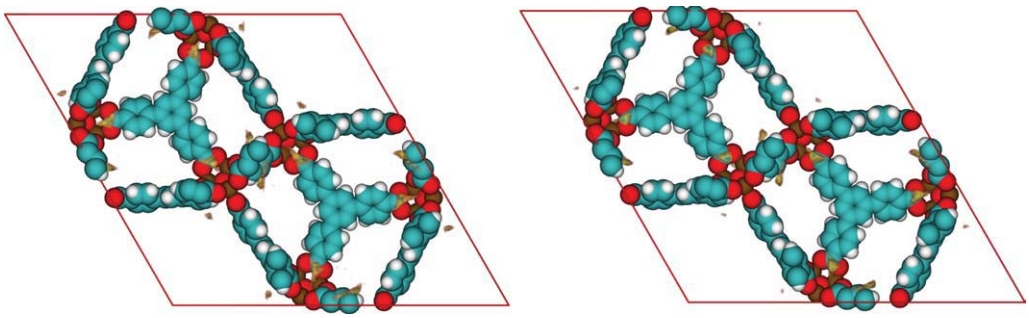

Figure 2. Density plots of mixture adsorption in UMCM-1 at 0.6 MPa and at 273 K for Kr (left) and Xe (right).

The majority of adsorption is near the Zn_4O corners and along the organic linkers. Before the simulation, the unit cell is divided into 150 × 150 × 150 voxels. After each cycle, the number of adsorbed molecules is counted, and their corresponding voxel values are updated accordingly. After normalization with respect to the highest occurring value in the histogram, the probability of finding an adsorbed molecule is represented in color. White and grey colors represent the least probable regions, and orange, yellow, and blue regions represent increasingly more probable regions. These colored regions are different from the framework atoms, whose carbon, hydrogen, oxygen, and zinc atoms are grey, white, red, and olive green, respectively. [Color figure can be viewed in the online issue, which is available at wileyonlinelibrary.com.]

We performed grand canonical Monte Carlo (GCMC) calculations to simulate adsorption in these MOFs.[31,32] A total of 50,000 equilibration cycles and 250,000 production cycles were used for each simulation. One cycle consists of N moves, where N is the number of molecules (minimum of 20 moves). Insertion, deletion, translation, and identity change moves (e.g., change Xe to Kr) were considered. By dividing the production run into five independent blocks and calculating the standard deviation of the block averages, an average error of 1.3% in the loading is estimated at the 95% confidence interval. Using propagation of error, the selectivities reported have estimated errors of 1.8% at the 95% confidence interval. Single-component and mixture isotherms were simulated for each MOF. The mixture isotherms had a fixed 80/20 molar composition of krypton to xenon in the gas phase to be representative of an industrial mixture. Fugacities were calculated using the Peng-Robinson equation of state. Framework atoms were considered fixed at their crystallographic coordinates. This approximation of a rigid framework has been shown to be a reasonable strategy for screening adsorption in MOFs.[22] A 12-6 Lennard-Jones potential was used to describe sorbate-framework interactions. For the MOF atoms, van der Waals parameters were taken from the DREIDING[33] forcefield and, if not available, from the Universal Forcefield (UFF)[34] forcefield. This choice of forcefield has been effective in past studies of hydrogen and methane adsorption in IRMOF-1,[35,36] and CO_2 adsorption in a variety of MOFs.[37,38] A cutoff of 1.2 nm was used for the van der Waals interactions. Krypton[39] and xenon[40] parameters were obtained from the literature. Lorentz-Berthelot mixing rules were used for the gas/framework interactions. No electrostatic charges were considered. Selectivities from the mixture isotherms were calculated with the standard definition:

$$\text{Selectivity} = (x_{\text{Xe}}/y_{\text{Xe}})/(x_{\text{Kr}}/y_{\text{Kr}})$$

where x_i is the adsorbed phase mole fraction of component i, and y_i is the gas phase mole fraction of component i. Additionally, in some cases, we crudely predicted selectivities of mixture adsorption from the single-component isotherms by calculating the ratio of the amount of adsorbed Xe at a given pressure to the amount of adsorbed Kr at the same pressure. All simulations were performed at 273 K. All data reported are excess adsorption isotherms, which can be calculated using absolute adsorption values, pore volume, and bulk fluid density.[41] Also, IAST calculations were performed to determine whether single-component isotherms could be used to predict accurately the results from full mixture simulations.

Results

IRMOF-1 (also known as MOF-5) is probably the most studied MOF to date. Our results for xenon and krypton adsorption in IRMOF-1 are comparable with the previous results from Greathouse et al.[22] (Supporting Information, Figure S2). Selectivities of ~3.5–4 for xenon over krypton are predicted, and this selectivity changes very little as a function of pressure. Adsorption in UMCM-1 also displays xenon selectivities of ~3.5–4, as shown in Figure 1. Although the capacity of UMCM-1 is by far the largest of all MOFs investigated here (~15 and 25 mol/kg in single-component isotherms for Kr and Xe, respectively), the xenon selectivity does not represent a significant improvement relative to previously reported values for zeolites. Density plots

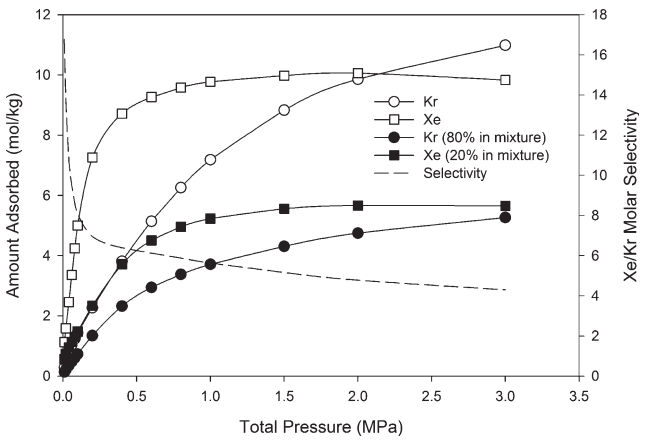

Figure 3. Single-component (open symbols) and mixture (filled symbols) isotherms for Xe and Kr adsorption in HKUST-1 at 273 K.

At low pressures (~0.01 MPa), the xenon selectivity is nearly 17, which is higher than the selectivities estimated from the single-component isotherms.

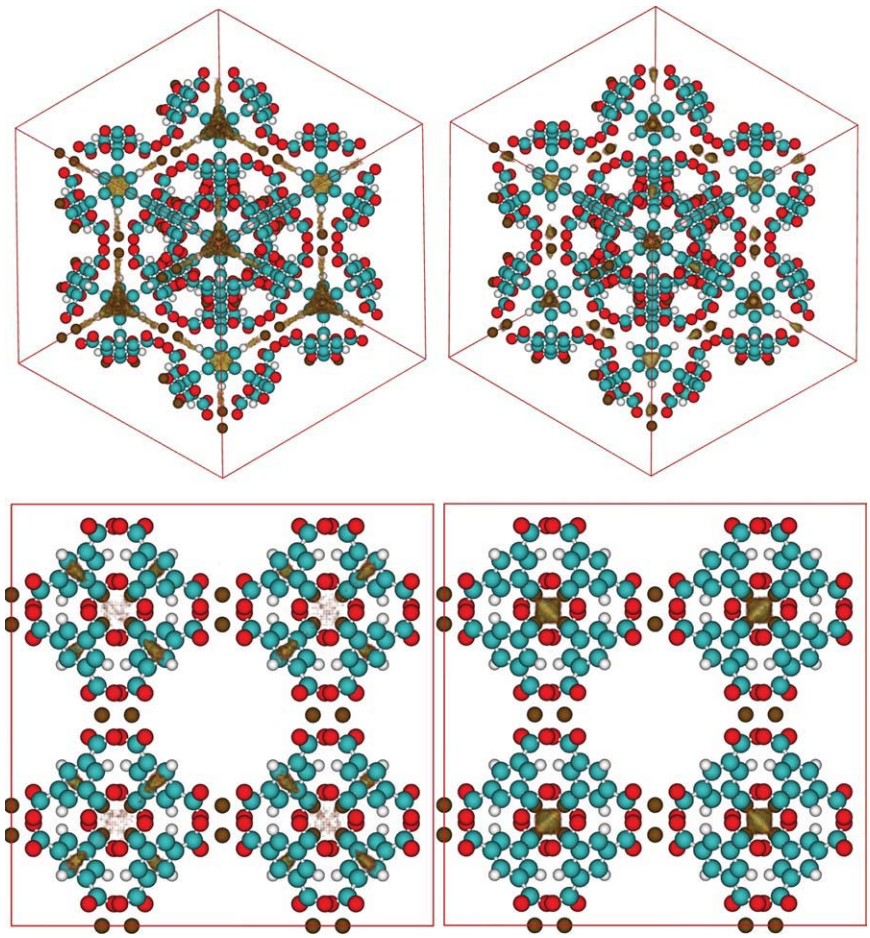

Figure 4. Single-component density plots of Kr (top left) and Xe (top right) in HKUST-1 at 0.1 MPa and at 273 K, as well as mixture density plots of Kr (bottom left) and Xe (bottom right).

The presence of Xe in the octahedral pockets of HKUST-1 prohibits Kr from adsorbing, leading to a significant enhancement in xenon selectivity. [Color figure can be viewed in the online issue, which is available at wileyonlinelibrary.com.]

at 0.6 MPa (Figure 2) suggest that xenon and krypton atoms adsorb next to organic linkers once stronger sites near the corners are filled, which is a mechanism that was previously found for other molecules in IRMOFs.[42] Additionally, crudely estimating selectivity of mixture adsorption from the single-component data allows one to obtain a good estimate of the xenon selectivity calculated explicitly from the mixture simulations. Adsorption in both IRMOF-1 and UMCM-1 follows IAST (Supporting Information, Figures S3 and S5). Given the relatively modest selectivities in these large-pore MOFs, we thought it would be beneficial to study MOFs with smaller pore sizes where there are stronger adsorption sites to enhance the selectivity.

This hypothesis is borne out by the mixture isotherms in ZIF-8 that show a maximum xenon selectivity of ~7 (Supporting Information, Figure S7). Its smaller pores yield stronger adsorption sites, which favor Xe binding and lead to an increase in selectivity. Figure S9 (Supporting Information) shows the heats of adsorption for single components in ZIF-8. The heats of adsorption rise for both Xe and Kr with increasing loading, due to the increasing importance of sorbate–sorbate interactions. Although the pores of ZIF-8 are smaller than those of IRMOF-1 and UMCM-1, the pore diameters of ZIF-8 are still large relative to the size of xenon and krypton (0.4100 and 0.3636 nm, respectively). This void space lacks adsorption sites that are strong enough to enhance xenon selectivity dramatically.

Figure 3 shows the calculated isotherms for HKUST-1, which was previously tested experimentally as an adsorbent material for Xe/Kr separation.[21] Although binary adsorption selectivities naively estimated from the single-component isotherms are between three and four at 0.1 MPa, mixture adsorption results predict much higher xenon selectivities: nearly 17 at 0.01 MPa and 8 at 0.1 MPa. Density plots shown in Figure 4 reveal the cause of this large selectivity at low coverage. In single-component adsorption, both Kr and Xe prefer to adsorb in the small octahedral pockets as they are the strongest adsorption sites in the MOF. These pockets are so small that only one atom of Xe or Kr can fit inside. However, when a binary mixture is present, xenon and krypton directly compete for these strong binding sites. At low loading, heats of adsorption for krypton and xenon have values of 21 and 32 kJ/mol, respectively, which represents a significant increase relative to their values at marginally higher loading (Figure 5). Because of stronger van der Waals interactions, xenon preferentially occupies this octahedral pocket and prevents krypton from

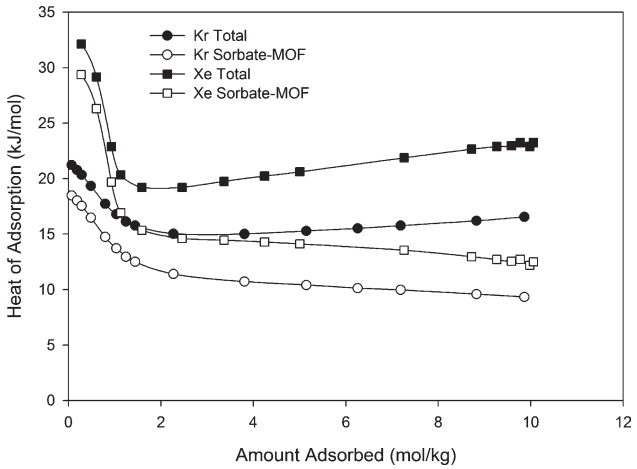

Figure 5. Heats of adsorption vs. loading for Kr (circles) and Xe (squares) single-component adsorption in HKUST-1 at 273 K, as well as the sorbate-MOF contribution.

At low loading, adsorption in the small octahedral pockets leads to high heats of adsorption.

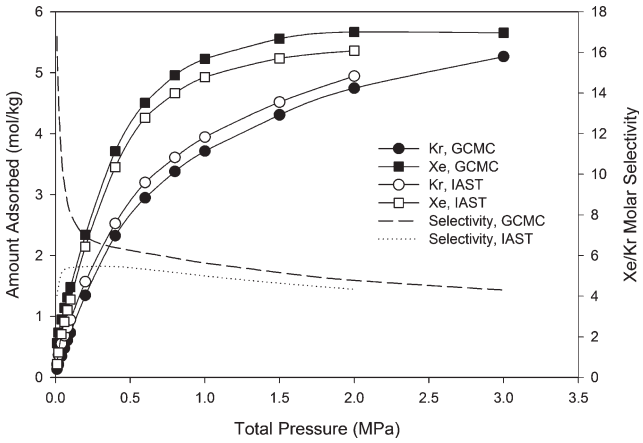

Figure 6. Mixture isotherms from GCMC simulations (filled symbols) and isotherms predicted by IAST based on single-component isotherms (open symbols) for Xe and Kr adsorption in HKUST-1 at 273 K.

IAST does not correctly predict Xe and Kr mixture selectivities at low loading as it cannot correctly capture competitive adsorption in the octahedral pockets.

adsorbing, as indicated by the lack of density inside these pockets for the mixture results in Figure 4. Instead, krypton adsorbs near the pocket openings. Adsorption in HKUST-1 leads to significant deviation from IAST, which predicts xenon selectivities between four and five as shown in Figure 6. This deviation is significant at low pressure, which is in contrast to most adsorption systems, where deviations from ideality are more common at higher loadings. We attribute this to the inability of IAST to capture the competitive sorption in the octahedral pockets.[43]

This phenomenon of high selectivity in very small pores has been previously investigated by Davis and coworkers in zeolites and idealized pore geometries. Van Tassel et al.[44] simulated Xe and Ar adsorption in NaA zeolite and found that xenon was favored both energetically and entropically at low loadings (low chemical potential) whereas argon was favored at high loadings (high chemical potential) as the smaller atoms could pack more efficiently into the pore volume. Keffer et al.[45] later simulated competitive xenon and argon adsorption in theoretical slit, cylindrical, and spherical nanopores and found that Xe was always selectively favored at low loadings over Ar as long as the pore was large enough to accommodate a Xe atom. Interestingly, in contrast to the zeolite results, imposing high chemical potentials did not always favor adsorption of the smaller argon atoms. They found that, at high chemical potential, a spherical pore whose diameter was comparable with that of xenon was occupied by over 99.4% xenon and resulted in a selectivity of 35.7.[45] Thus, pore confinement had a substantial impact on the adsorptive selectivity.

It is reasonable to expect that these same concepts can be applied to picking candidate MOFs for Xe/Kr separation. Thus, we propose that MOFs with adsorption sites that are large enough to accommodate a Xe atom but small enough to fit only one atom are attractive candidates. For example, although HKUST-1 showed preferential adsorption sites, the xenon selectivity considerably drops from 17 at 0.01 MPa to 8 at 0.1 MPa and nearly approaches that predicted by IAST at ~1.0–1.5 MPa because of increased adsorption in the larger pores. These results show that although adsorption in the octahedral pockets is highly nonideal, adsorption in the larger pores is ideal and increasingly contributes to the overall xenon selectivity as the pressure and gas loading are increased. Therefore, we examined other MOFs to identify those with smaller pores that also impart nonideal adsorption and maintain enhanced xenon selectivity over a wider pressure range.

One attractive candidate was MOF-505, which has smaller average pore sizes than HKUST-1. The simulation results for this MOF are shown in Figure 7. The steepness of the single-component isotherms indicates that small pores are present and that adsorbed species have high heats of adsorption. Density plots reveal adsorption of xenon and krypton

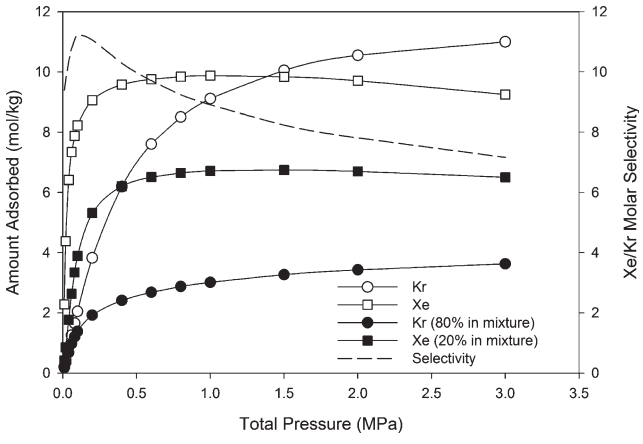

Figure 7. Single-component (open symbols) and mixture (filled symbols) isotherms for Xe and Kr adsorption in MOF-505 at 273 K.

Unlike HKUST-1, xenon selectivity remains elevated even at higher pressures, making it a promising candidate material for Xe/Kr separation.

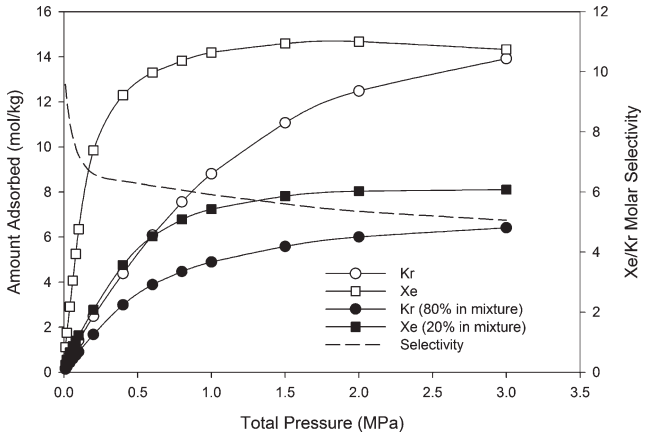

Figure 8. Single-component (open symbols) and mixture (filled symbols) isotherms for Xe and Kr adsorption in NOTT-101 at 273 K.

The extra phenyl moiety in the linker compared with MOF-505 makes the pore size too large and leads to lower selectivities relative to those predicted for MOF-505.

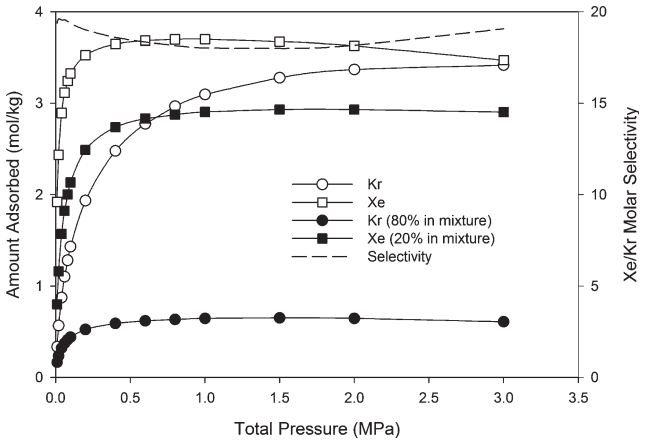

Figure 9. Single-component (open symbols) and mixture (filled symbols) isotherms for Xe and Kr adsorption in Pd-MOF at 273 K.

near the pore openings in the MOF (Supporting Information, Figure S12). Compared with HKUST-1, MOF-505 has a smaller cavity size, which allows the xenon selectivity to remain elevated over a wide pressure range (~9 at 1 MPa). As typical pressure swing adsorption processes run between 0.1 and 0.5 MPa, the selectivities of MOF-505 of ~10–11 in this pressure range are superior to those of HKUST-1 (~6–8), making MOF-505 a more attractive MOF for Xe/Kr separation. To explore whether the enhanced selectivity of MOF-505 was due to pore size and not to framework topology, NOTT-101 and NOTT-108 were tested. These MOFs have the same topology as MOF-505 but are composed of slightly longer triphenyl linkers. Figure 8 shows that the results follow a similar trend to those for HKUST-1, where a maximum selectivity of about 10 occurs at 0.01 MPa for the mixture isotherms and then decreases significantly with increasing pressure and gas loading (down to 5 at 3 MPa). The pore sizes of NOTT-101 are too large to ensure nonideal adsorption at higher loadings. The results for NOTT-108 can be interpreted similarly and are not significantly different from those for NOTT-101 despite the presence of fluorine atoms on the organic linkers (Supporting Information, Figure S15).

Finally, we investigated Pd-MOF to test MOFs with even smaller pores. Figure 9 displays the simulation results. The pores are so small that the xenon selectivity is very high, remaining near 18 or 19 for the entire pressure range from 0.01 to 3 MPa. Density plots (Figure 10) reveal that Xe and Kr can only adsorb in the larger cavities of the MOF and not in the octahedral pockets, which are too small. Xenon dominates the adsorption at all pressures and prevents krypton from adsorbing, leading to the high selectivity. However, the adsorption capacities of both Xe and Kr are significantly lower than those of the other MOFs. In fact, Pd-MOF had the lowest void fraction (0.348) of all MOFs investigated. These results offer a preliminary estimate to the maximum xenon selectivity using competitive adsorption sites in MOFs.

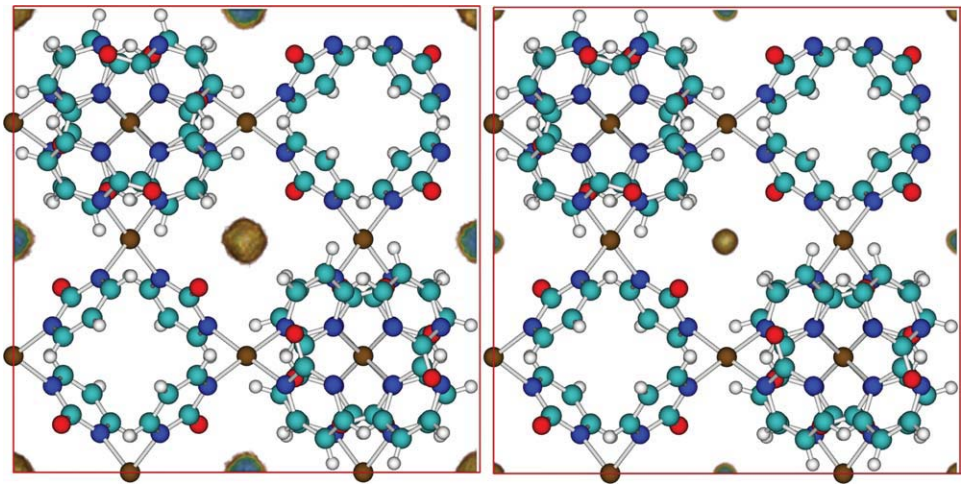

Figure 10. Mixture density plots of Kr (left) and Xe (right) in Pd-MOF at 0.4 MPa and at 273 K.

[Color figure can be viewed in the online issue, which is available at wileyonlinelibrary.com.]

Table 2. Xe/Kr Selectivity for All MOFs Investigated at Pressures of 0.01 MPa, 0.1 MPa, and 1 MPa as Predicted from Mixture Simulations at 273 K

	Xe/Kr Selectivity		
MOF	0.01 Mpa	0.1 Mpa	1 Mpa
IRMOF-1	3.6	3.7	4.1
UMCM-1	3.5	3.6	3.7
ZIF-8	6.5	6.8	5.6
HKUST-1	16.8	8.1	5.6
MOF-505	9.4	11.2	8.9
NOTT-101	9.6	7.2	5.9
NOTT-108	11.0	7.7	6.1
Pd-MOF	19.4	19.4	18.0

Conclusions

We have performed GCMC simulations of both single component and mixture adsorption of Xe and Kr in a variety of MOFs. The results are summarized in Table 2. Pd-MOF is predicted to have the largest selectivity, and the high selectivity is maintained across a wide range of pressures in this material. Large pore materials are not desirable for efficient Xe/Kr separation. Both IRMOF-1 and UMCM-1 show low xenon selectivities of about four and follow ideal adsorption. To enhance selectivity, small pores or pockets are needed to preferably bind Xe instead of Kr and introduce nonideality to mixture adsorption. HKUST-1 has a high adsorptive selectivity at low loading due to its small pockets where Xe atoms adsorb with higher heats of adsorption than Kr. However, the selectivities in HKUST-1 drop off quickly at higher pressure due to the presence of large cavities, which are filled after the small octahedral pockets, demonstrating that the best MOFs for Xe/Kr separation should have uniformly small cavity sizes without additional large cavities. MOF-505 has two types of pores, but both are relatively small, and the MOF maintains its elevated xenon selectivities over a large pressure range. NOTT-101 and NOTT-108 share the same topology with MOF-505 but have pores that are too large for efficient Xe/Kr separation. We are currently working to validate our theoretical results with adsorption experiments.

Acknowledgments

This research was supported by a 3M Fellowship and by the Chemical Sciences, Geosciences, and Biosciences Division, Office of Basic Energy Sciences, Office of Science, U.S. Department of Energy, Grant No. DE-FG02-03ER15457. This research used resources of the National Energy Research Scientific Computing Center, which is supported by the Office of Science of the U.S. Department of Energy under Contract No. DE-AC02-05CH11231. The authors thank Prof. Joseph Hupp for helpful discussions.

Literature Cited

1. Kerry FG. *Industrial Gas Handbook: Gas Separation and Purification*. Boca Raton, Florida: CRC Press, 2007.
2. Izumi J.*Waste gas treatment using zeolites in nuclear-related industries*. In: Auerbach SM, Carrado KA, Dutta PK, editors. *Handbook of Zeolite Science and Technology*. New York: Marcel Dekker, 2003.
3. Jameson CJ, Jameson AK, Lim HM. Competitive adsorption of xenon and krypton in zeolite NaA: Xe-129 nuclear magnetic resonance studies and grand canonical Monte Carlo simulations. *J Chem Phys*. 1997;107:4364–4372.
4. Rowsell JLC, Yaghi OM. Metal-organic frameworks: a new class of porous materials. *Microporous Mesoporous Mater*. 2004;73:3–14.
5. Ferey G. Hybrid porous solids: past, present, future. *Chem Soc Rev*. 2008;37:191–214.
6. Kitagawa S, Kitaura R, Noro S. Functional porous coordination polymers. *Angew Chem Int Ed Engl*. 2004;43:2334–2375.
7. Rowsell JL, Yaghi OM. Strategies for hydrogen storage in metal-organic frameworks. *Angew Chem Int Ed Engl*. 2005;44:4670–4679.
8. Hirscher M, Panella B. Hydrogen storage in metal-organic frameworks. *Scr Mater*. 2007;56:809–812.
9. Murray LJ, Dinca M, Long JR. Hydrogen storage in metal-organic frameworks. *Chem Soc Rev*. 2009;38:1294–1314.
10. Liu B, Yang Q, Xue C, Zhong C, Chen B, Smit B. Enhanced adsorption selectivity of hydrogen/methane mixtures in metal-organic frameworks with interpenetration: a molecular simulation study. *J Phys Chem C*. 2008;112:9854–9860.
11. Li JR, Kuppler RJ, Zhou HC. Selective gas adsorption and separation in metal-organic frameworks. *Chem Soc Rev*. 2009;38:1477–1504.
12. Lee J, Farha OK, Roberts J, Scheidt KA, Nguyen ST, Hupp JT. Metal-organic framework materials as catalysts. *Chem Soc Rev*. 2009;38:1450–1459.
13. Shultz AM, Farha OK, Hupp JT, Nguyen ST. A catalytically active, permanently microporous MOF with metalloporphyrin struts. *J Am Chem Soc*. 2009;131:4204–4205.
14. Cho SH, Ma BQ, Nguyen ST, Hupp JT, Albrecht-Schmitt TE. A metal-organic framework material that functions as an enantioselective catalyst for olefin epoxidation. *Chem Commun*. 2006:2563–2565.
15. Bae YS, Mulfort KL, Frost H, Ryan P, Punnathanam S, Broadbelt LJ, Hupp JT, Snurr RQ. Separation of CO_2 from CH_4 using mixed-ligand metal-organic frameworks. *Langmuir*. 2008;24:8592–8598.
16. Bae YS, Farha OK, Hupp JT, Snurr RQ. Enhancement of CO_2/N_2 selectivity in a metal-organic framework by cavity modification. *J Mater Chem*. 2009;19:2131–2134.
17. Pan L, Olson DH, Ciemnolonski LR, Heddy R, Li J. Separation of hydrocarbons with a microporous metal-organic framework. *Angew Chem Int Ed Engl*. 2006;45:616–619.
18. Hartmann M, Kunz S, Himsl D, Tangermann O, Ernst S, Wagener A. Adsorptive separation of isobutene and isobutane on $Cu_3(BTC)_2$. *Langmuir*. 2008;24:8634–8642.
19. Yang QY, Zhong CL. Molecular simulation of carbon dioxide/methane/hydrogen mixture adsorption in metal-organic frameworks. *J Phys Chem B*. 2006;110:17776–17783.
20. Yang QY, Xue CY, Zhong CL, Chen JF. Molecular simulation of separation of CO_2 from flue gases in Cu-BTC metal-organic framework. *AlChE J*. 2007;53:2832–2840.
21. Mueller U, Schubert M, Teich F, Puetter H, Schierle-Arndt K, Pastre J. Metal-organic frameworks- prospective industrial applications. *J Mater Chem*. 2006;16:626–636.
22. Greathouse JA, Kinnibrugh TL, Allendorf MD. Adsorption and separation of noble gases by IRMOF-1: Grand canonical Monte Carlo simulations. *Ind Eng Chem Res*. 2009;48:3425–3431.
23. Eddaoudi M, Kim J, Rosi N, Vodak D, Wachter J, O'Keeffe M, Yaghi OM. Systematic design of pore size and functionality in isoreticular MOFs and their application in methane storage. *Science*. 2002;295:469–472.
24. Koh K, Wong-Foy AG, Matzger AJ. A crystalline mesoporous coordination copolymer with high microporosity. *Angew Chem Int Ed Engl*. 2008;47:677–680.
25. Park KS, Ni Z, Cote AP, Choi JY, Huang RD, Uribe-Romo FJ, Chae HK, O'Keeffe M, Yaghi OM. Exceptional chemical and thermal stability of zeolitic imidazolate frameworks. *Proc Natl Acad Sci USA*. 2006;103:10186–10191.
26. Chui SSY, Lo SMF, Charmant JPH, Orpen AG, Williams ID. A chemically functionalizable nanoporous material $[Cu_3(TMA)_2(H_2O)_3]_n$. *Science*. 1999;283:1148–1150.
27. Chen BL, Ockwig NW, Millward AR, Contreras DS, Yaghi OM. High H_2 adsorption in a microporous metal-organic framework with open metal sites. *Angew Chem Int Ed Engl*. 2005;44:4745–4749.
28. Lin X, Telepeni I, Blake AJ, Dailly A, Brown CM, Simmons JM, Zoppi M, Walker GS, Thomas KM, Mays TJ, Hubberstey P, Champness NR, Schroder M. High capacity hydrogen adsorption in Cu(II) tetracarboxylate framework materials: the role of pore size,

ligand functionalization, and exposed metal sites. *J Am Chem Soc*. 2009;131:2159–2171.
29. Xamena FXLI, Abad A, Corma A, Garcia H. MOFs as catalysts: activity, reusability and shape-selectivity of a Pd-containing MOF. *J Catal*. 2007;250:294–298.
30. Bohlmann W, Poppl A, Sabo M, Kaskel S. Characterization of the metal-organic framework compound Cu_3(benzene 1,3,5-tricarboxylate)$_2$ by means of ^{129}Xe nuclear magnetic and electron paramagnetic resonance spectroscopy. *J Phys Chem B*. 2006;110:20177–20181.
31. Snurr RQ, Yazaydin AO, Dubbeldam D, Frost H. *Molecular modeling of metal-organic frameworks*. In: MacGillivray L, editor. *Metal-Organic Frameworks: Design and Application*: Hoboken, NJ: Wiley-VCH,2010.
32. Düren T, Bae YS, Snurr RQ. Using molecular simulation to characterise metal-organic frameworks for adsorption applications. *Chem Soc Rev*. 2009;38:1237–1247.
33. Mayo SL, Olafson BD, Goddard WA. Dreiding—a generic force-field for molecular simulations. *J Phys Chem*. 1990;94:8897–8909.
34. Rappe AK, Casewit CJ, Colwell KS, Goddard WA, Skiff WM. UFF, a full periodic-table force-field for molecular mechanics and molecular-dynamics simulations. *J Am Chem Soc*. 1992;114:10024–10035.
35. Ryan P, Broadbelt LJ, Snurr RQ. Is catenation beneficial for hydrogen storage in metal-organic frameworks? *Chem Commun*. 2008:4132–4134.
36. Düren T, Sarkisov L, Yaghi OM, Snurr RQ. Design of new materials for methane storage. *Langmuir*. 2004;20:2683–2689.
37. Walton KS, Millward AR, Dubbeldam D, Frost H, Low JJ, Yaghi OM, Snurr RQ. Understanding inflections and steps in carbon dioxide adsorption isotherms in metal-organic frameworks. *J Am Chem Soc*. 2008;130:406–407.
38. Yazaydin AO, Benin AI, Faheem SA, Jakubczak P, Low JJ, Willis RR, Snurr RQ. Enhanced CO_2 adsorption in metal-organic frameworks via occupation of open-metal sites by coordinated water molecules. *Chem Mater*. 2009;21:1425–1430.
39. Talu O, Myers AL. Reference potentials for adsorption of helium, argon, methane, and krypton in high-silica zeolites. *Colloids Surf A*. 2001;187:83–93.
40. Hirschfelder JO, Curtiss CF, Bird RB. *Molecular Theory of Gases and Liquids*. New York: Wiley, 1965.
41. Myers AL, Monson PA. Adsorption in porous materials at high pressure: theory and experiment. *Langmuir*. 2002;18:10261–10273.
42. Frost H, Düren T, Snurr RQ. Effects of surface area, free volume, and heat of adsorption on hydrogen uptake in metal-organic frameworks. *J Phys Chem B*. 2006;110:9565–9570.
43. Murthi M, Snurr RQ. Effects of molecular siting and adsorbent heterogeneity on the ideality of adsorption equilibria. *Langmuir*. 2004;20:2489–2497.
44. van Tassel PR, Davis HT, McCormick AV. Adsorption simulations of small molecules and their mixtures in a zeolite micropore. *Langmuir*. 1994;10:1257–1267.
45. Keffer D, Davis HT, McCormick AV. Effect of loading and nanopore shape on binary adsorption selectivity. *J Phys Chem*. 1996;100:638–645.

Manuscript received Jun. 21, 2010, and revision received Aug. 3, 2010.